Eur. Phys. J. E **22**, 201–208 (2007)
DOI: 10.1140/epje/e2007-00023-0

THE EUROPEAN PHYSICAL JOURNAL E

Initiation and evolution of current ripples on a flat sand bed under turbulent water flow

V. Langlois[1,a] and A. Valance[2,b]

[1] School of Physics, Trinity College Dublin, Dublin 2, Ireland
[2] G.M.C.M., Université Rennes 1, Bât. 11A, 35042 Rennes, France

Received 4 December 2006 / Received in final form 14 February 2007
Published online: 21 March 2007 –

Abstract. We investigate the formation and dynamics of sand ripples under a turbulent water flow. Our experiments were conducted in an open flume with spherical glass beads between 100 and 500 μm in diameter. The flow Reynolds number is of the order of 10 000 and the particle Reynolds number of the order of 1 to 10. We study the development of ripples by measuring their wavelength and amplitude in course of time and investigate the influence of the grain size and the flow properties. In particular, we demonstrate two different regimes according to the grain size. For fine grains, a slow coarsening process (i.e., a logarithmic increase of the wavelength and amplitude) takes place, while for coarser grains, this process occurs at a much faster rate (i.e., with a linear growth) and stops after a finite time. In the later case, a stable pattern is eventually observed. Besides, we carefully analyze the wavelength of ripples in the first stages of the instability as a function of the grain size and the shear velocity of the flow, and compare our results with other available experimental data and with theoretical predictions based on linear stability analyses.

PACS. 45.70.-n Granular systems – 45.70.Qj Pattern formation – 92.10.Wa Sediment transport

1 Introduction

Ripples are one of the most common patterns created by the interaction between a granular material and a moving fluid [1,2]. In natural environments sand ripples can be of three different types, depending on the external conditions: aeolian ripples (driven by the wind), sea-wave ripples (oscillatory water flow) or current ripples (unidirectional water flow). The same type of flows of particle-charged fluids are also common in industrial transport processes, where problems can arise from the development of bedforms through the section of a pipe. In every case the mechanisms are similar: the bedforms emerge from the transport of grains by the fluid on the surface of the sediment layer. In this paper we will focus only on the case of the subaqueous ripples under a steady flow.

Although these patterns have been the subject of many theoretical and experimental works, some questions remain unanswered. Amongst these are the differences between the mechanisms in the laminar and turbulent cases, and the question of the long-time evolution of the ripples. The first attempts of modeling the ripple formation have been based on the turbulent case, such as in [3–5]. Indeed the flows encountered in nature are mostly turbulent. In these models, the turbulent flow close to the bed is described via a height dependent eddy-viscosity approach and combined to a transport law. However, the assumption that the turbulence is necessary to the initiation of ripples has been proven wrong. Charru et al. [6] showed that if the viscous and inertial effects of the fluid are taken into account, a flat sand bed is unstable even in laminar conditions, which has been confirmed by several experimental studies. However, if the study of a laminar flow is easier, it is worth noting that obtaining ripples while remaining in the laminar regime requires practical limitations: the Shields number has to be high enough for the sediment to be transported by the fluid, whereas on the other hand the Reynolds number must be small enough to avoid turbulence. To fulfill both conditions, laminar experiments have been conducted either in quasi-2D Hele-Shaw cells [7], in very shallow annular channels [8] or with fluids more viscous than water [9].

Yet obtaining a correct prediction of the ripple wavelength is still a challenging problem, whether it is under a laminar or turbulent flow. Most traditional stability analysis leads commonly to an underestimated prediction of the wavelength. Recently, several attempts have been made to better describe the bedload transport process. The recent works by Charru et al. [6] tried to model more precisely the sediment transport by incorporating results of the viscous resuspension theory by Leighton and Acrivos [10].

[a] e-mail: vincent.langlois@tcd.ie
[b] e-mail: alexandre.valance@univ-rennes1.fr

However, this theory applied in the case of a laminar flow still fails to predict a correct value of the wavelength at the initiation of the instability. More recently, Valance [11,12] inspiring from works on aeolian transport [13,14] introduced a new characteristic length scale in the sand transport process, that is the length needed for the sand flux to equilibrate with the fluid flow. This new length appears to control the most unstable wavelength, and the predicted value is more compatible with usual observations. However, as emphasized by Coleman and Melville [15], despite the huge number of sand ripple experiments in water reported in the literature, only a few of them can be used for a comparison with the predictions of stability analysis. Indeed, most of the experimental data concern the equilibrium bedforms which are observed at long times after a nonlinear transient. These patterns differ markedly from those observed at the first stages of the ripple development. In particular, the wavelength of the final bedform is usually much larger than that of the ripple pattern at the initiation of the instability. This is the case in particular for the data gathered by Yalin [16], where the reported ripple wavelengths are unusually large (typically $\lambda/d \sim 1000$) compared to other measurements. In other cases, the hydraulic conditions were not carefully measured or reported. Hereafter, we will refer to the wavelength of the ripple pattern at the very first stages of its development as the initial wavelength.

Another classical unsolved issue is the eventual evolution of the bedforms. Different experimental studies gave various results: Betat et al. [8,17] observed in an annular 2D channel a stabilization of both the amplitude and the wavelength of the ripples after a long time. In a laminar 2D flume, Loiseleux et al. [7], on the contrary, observed no saturation: the ripples keep growing with time. The three-dimensional case appears to be even more complicated, since the bedforms usually loose their translational invariance in the transverse direction and exhibit more complex patterns [18]. A few numerical attempts have been performed in order to understand the coarsening phenomenon. It is necessary to go beyond the linear approximations used for the stability analysis. However, the complete numerical calculation of the fluid flow at each step over a moving bed is still too demanding in computational time. Therefore approximations have been used. A typical result is that the only existence of a threshold in the transport law is sufficient for the system to exhibit a coarsening process. Results by Lagrée [19] show a linear increase of the average wavelength with time. This coarsening appears to cease only when there is only a single large ripple left in the computational domain. To date no physical mechanism outside the influence of the finite-size of the system has been exhibited to account for a possible saturation of the coarsening process.

The aim of the experimental study presented in this article is to provide precise measurements of both the wavelength and amplitude of ripples during their temporal evolution. These measurements were performed in a three-dimensional water flume, in which the properties of the flow have been carefully characterized. We varied the shear velocity of the flow from 1 to 2 cm/s and used three different grain sizes (100, 250 and 500 μm).

The paper is organized as follows: in Section 2 we detail the experimental set-up and procedure used to characterize the ripple pattern, and we focus on the measured characteristics of the water flow. In Section 3, we first present the results concerning the temporal evolution of the wavelength and amplitude of the ripple pattern. We then focus on the wavelength at the initiation of the instability and investigate the influence of the grain size and shear velocity of the flow. In Section 4, the results are discussed and compared with theoretical predictions. Finally, conclusion and prospects are given in Section 5.

2 Experimental set-up

2.1 Water flume

Our experimental set-up consists of a 3 m long open flume, with a 120 mm $\times$ 75 mm rectangular section (Fig. 1). Every walls of the channel are made of transparent plexiglass for visualization. The bottom of the flume is filled with glass beads (volumic mass $\rho_g = 2.5 \times 10^3$ kg m^{-3}) of three diameter ranges: 70–110 μm, 200–300 μm and 400–600 μm. The fluid flow is supplied by a water tank installed 3 m above the flume. The level of water in the reservoir is kept constant so that the discharge can be easily controlled by a vane. The flow rate is measured before the entrance of the flume by an electromagnetic flow meter. After the junction between the pipe and the flume itself, the latter is filled over 20 cm with 1 cm wide glass beads in order to break the eddies induced by the section change. The flow is then channelized by a network of straws parallel to the flume.

The bed elevation is measured by a laser telemeter carried by a motorized rail over the length of the flume. The telemeter has a resolution of 10 μm when used for detecting the displacement of a smooth surface. In the case of a granular surface, the resolution is much less (of order of a few tenth of millimeters) because of the diffusion of the laser beam inside the bed. This set-up allows to measure the height profile of the ripples on several sections across the channel width. However, we did not perform measurements closer than 10 mm from the lateral walls. Our procedure to study the growth of the ripples is the following: the granular bed is carefully flattened before the flow. In a first step, the flume is filled with water. The flow rate is then slowly increased while kept under the movement threshold. Finally, it is rapidly increased to the required value with a ramp of 1 s. In order to perform measurements of the bed topography, the flow rate is decreased under the threshold of sand transport to "freeze" the ripple evolution during the measure. We verified by comparing to the results of continuous experiments, that multiple pauses in the process did not affect the statistical properties of the ripples over time.

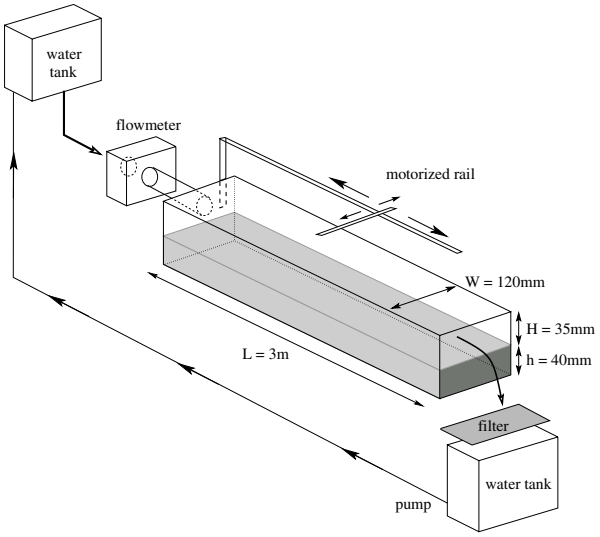

Fig. 1. Schematic representation of the experimental set-up. The flume is covered by a lid so that the flow has no free surface. Its dimensions are $L = 3$ m, $W = 120$ mm, water depth $W = 35$ mm and sand bed thickness $h = 40$ mm.

2.2 Characterization of the flow

To analyze the characteristics of the flow in the experimental flume, we performed P.I.V. (Particle Imaging Velocimetry) measurements of the velocity field in the water, in absence of any sand grains or relief. Instead of the granular bed, a smooth bottom has been used. The fluid movement is traced by injection in the flow of 20 μm diameter hollow spheres, with a density equal to that of water. Images taken by a high-speed camera are then processed by cross-correlation to give the velocity field.

Figure 2a shows the time-averaged profiles of the horizontal velocity of the fluid in the central section of the flume, one meter away from the entrance. Once normalized by the value of the flow rate, these profiles collapse on the same curve, which proves that the flow is fully developed at this point. This can be theoretically verified: it is known that the thickness of the turbulent boundary layer grows with the distance like [20]

$$\delta(x) = 0.37\, x^{4/5} \left(\frac{U_\infty}{\nu}\right)^{-1/5} . \qquad (1)$$

The turbulent flow is considered to be fully developed when the width of the boundary layer is of order of half the height of the channel (hence the two boundary layers (upper and bottom) invade the whole height of the flow). Applying this criterion to our experimental parameters gives for the development length a typical value of 50 cm, which is less than the distance we allow between the flume entrance and our measurement zone. The vertical asymmetry of the flow profile, probably due to the entry conditions, should not interfere with the dynamics of the ripples, since these structures are always included in the lower part of the turbulent boundary layer. Let us remind that the top of the channel is covered by a Plexiglas

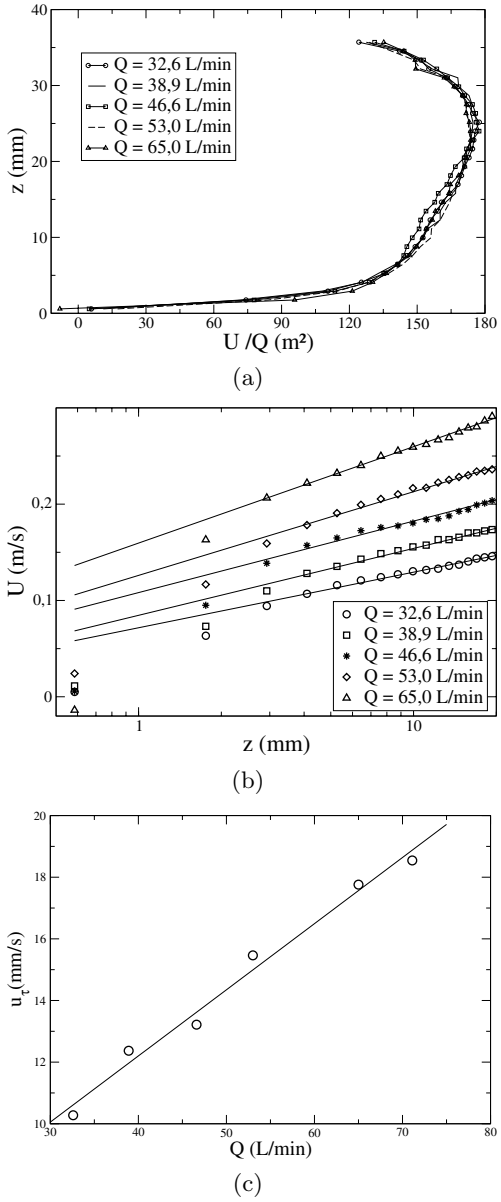

Fig. 2. (a) Average vertical profile of the horizontal velocity, normalized by the value of the flow rate. (b) Profiles of the horizontal velocity in semi-logarithmic scale. (c) Shear velocity as a function of the flow rate in the flume.

lid, so that the flow never presents any free surface. Thus we avoid any possible interaction between the sand waves and the free-surface disturbances (which may also be responsible for the formation of *dunes* or *anti-dunes*) [21]. In Figure 2b, we plotted the same velocity profiles in a semi-logarithmic scale. The center of the flume is characterized, as predicted by the classical turbulence theory, by a logarithmic profile:

$$U(z) = \frac{u_\tau}{\kappa} \ln\left(\frac{z}{z_0}\right) \qquad (2)$$

where u_τ is the friction velocity, $\kappa = 0.41$ the von Kármán constant, and z_0 the hydraulical roughness of the surface.

For a smooth wall, $z_0 = \nu/15u_\tau$, while for a wall made rough with glued grains, $z_0 = d/30$ (where d is the grain diameter). Note that close to the bottom wall, the data fall below the logarithmic fit: this is the signature of the presence of the sub-viscous layer. The value of the friction velocity is given by the slope of the logarithmic fit of Figure 2b, which allows us to calculate a particle Reynolds number

$$Re_\mathrm{p} = \frac{u_\tau d}{\nu}. \quad (3)$$

The linear relation between the value of u_τ and the direct control parameter, the flow rate, allows us to control easily the value of the particle Reynolds number of an experiment. The maximal value of the particle Reynolds number which is accessible in our flume varies between $Re_\mathrm{p} \sim 1$ for the 100 μm grains and $Re_\mathrm{p} \sim 15$ for the 500 μm grains.

It is worth noting that for each size of grains and the whole available range of flow rates, the fluid remains clear: the particles are moving only by rolling and hoping along the surface, without going into suspension in the core of the flow. The sediment transport is then entirely taken in charge by the bedload. Let us note that smaller grains (<100 μm) would be transported by suspension whereas our hydraulic set-up does not permit to reach the movement threshold for larger grains (>500 μm).

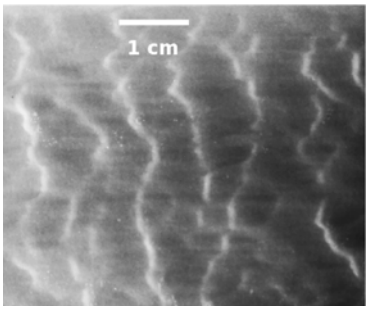

(a)

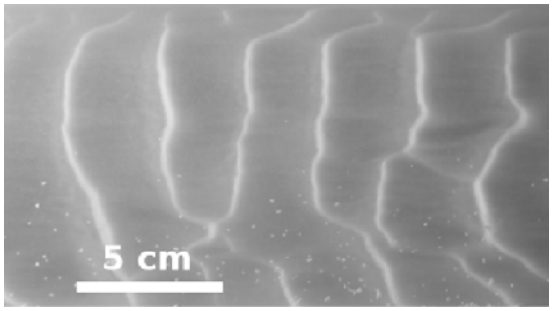

(b)

Fig. 3. Aspect of the ripples for $d = 100$ μm after (a) 1 min; (b) 4 min of erosion.

3 Experimental observations

Within a few minutes after the beginning of the experiment, the flat sand bed presents some disturbances: preliminary ripple patterns appear. The crests of ripples are first wavy and irregular (see Fig. 3a) and rapidly merge into well-defined two-dimensional ripples (that is, having straight crests perpendicular to the main flow) with a larger wavelength.

3.1 Evolution of ripples: coarsening process

During their evolution, the ripples migrate downstream and grow both in amplitude and wavelength. It is also remarkable that they become rapidly laterally asymmetric, which leads to more complex, three-dimensional patterns, like it was already observed, for instance by Baas [18]. This evolution explains the increasing dispersion in ripple wavelength and amplitude when measured on a straight line (as shown in Fig. 4), and ultimately makes it difficult to define significatively an average wavelength of the patterns. To our knowledge, no quantitative theoretical explanation of this transition towards 3D patterns has been proposed so far. Indeed the 3D stability analysis performed in the case of a laminar flow [22] shows that the most unstable mode always correspond to ripples perpendicular to the main flow. Moreover, numerical simulations based on a weakly non-linear analysis [23] tend to show that 3D structures are unstable and evolve towards 2D ripple patterns (i.e., translationally invariant in the transverse direction). However, in our experiment the presence

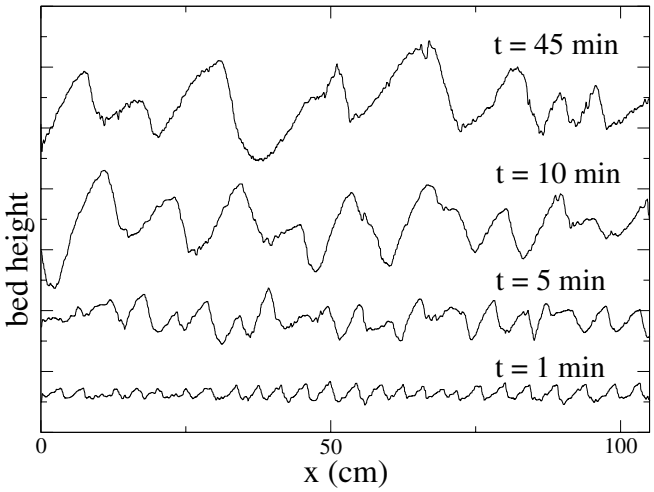

Fig. 4. Profile of the bed elevation in the central section of the flume at different times. $d = 250$ μm, $Re_p = 5.5$.

of the two lateral walls could have a non negligible influence and trigger the development of 3D patterns with a mechanism analog to that of the formation of alternate sand bars [24].

Figure 5a shows the temporal evolution of the height of the ripples during a given experiment using fine grains. The average amplitude of the ripples is defined as $\sqrt{\langle h(x)^2\rangle - \langle h(x)\rangle^2}$ where h is the height of the ripples. This evolution can be very well fitted by a logarithmic law. After one hour of running time, we do not observe any saturated state and the amplitude of the ripple keeps growing with time. Unfortunately, the finite length of our

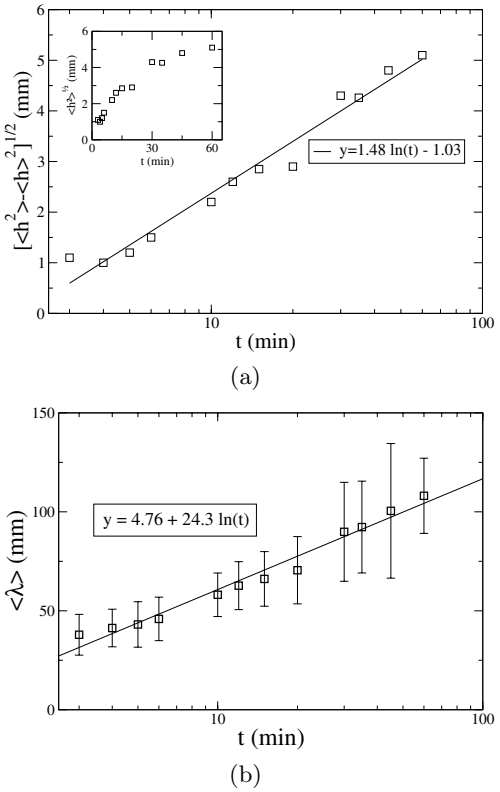

Fig. 5. Evolution of the average ripple amplitude (a), and wavelength (b) in logarithmic scales. $d = 100\,\mu$m, $Re_p = 2.2$.

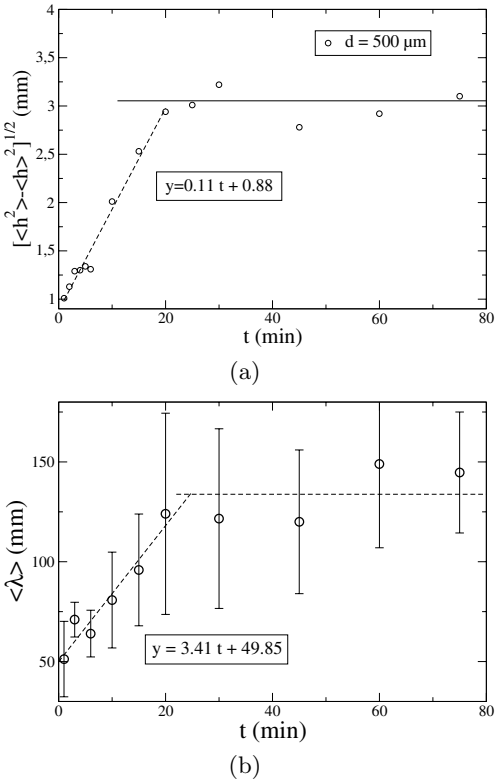

Fig. 6. Evolution of the average ripple amplitude (a) and wavelength (b) for $d = 500\,\mu$m and $Re_p = 13.5$.

flume and the finite amount of grains do not allow us to run the experiment over longer times, such as several hours or the whole day. Note also that the time needed for a ripple to go from one end of the flume to the other is about 3 h. This time, which is rather long due to the coarsening process resulting in a decrease of the ripple drift speed in course of time, determines the maximum duration for a relevant experiment. Betat et al. observed in an quasi-2D annular flume [17], with 290 μm beads, an equilibrium state after several days. In the experiments of Betat et al. [17], the total height of water is around 15 mm and the ripples reach 7 mm in amplitude. The saturation observed by Betat et al. could then be due to the strong confinement of the bedforms. In our experiment, the rms of the ripple profile is 5 mm after 1 h and is still small compared with the effective flow height (25 mm). Let us also mention observations by Loiseleux et al. [7] for quasi-2D ripples sheared by a laminar flow, which also show a logarithmic growth of their height at long times, with 110 μm glass beads. The wavelength of the fine grain ripples increases, as well, logarithmically in course of time (see Fig. 5b). This logarithmic coarsening is again also observed by Loiseleux et al. [7] and by Rousseaux et al. for ripples formed in a oscillatory flow [25].

For coarse grains (i.e., $d = 500\ \mu$m), we observe a different temporal evolution, as can be seen in Figure 6. In this case, the ripple amplitude and wavelength both increase linearly with time over a finite time, and then the coarsening interrupts. The system reaches a stable final state after approximately 20 min. Let us insist on the fact that in our experiments the maximal amplitude reached by the ripples in this case is still smaller than the maximal one observed for the finer beads. This observation may suggest that in our experiment the saturation of the ripples in amplitude is not directly related to the presence of the upper wall. An other physical mechanism explaining this process is thus still to be found.

3.2 First instants of the instability

While the theoretical studies of ripple coarsening remain sparse, many analytical attempts have been performed to model the initial growth of current ripples by investigating the linear stability of a flat sand bed, thus predicting the wavelength which is expected to appear in the first instants. In order to compare with these theoretical predictions, we now concentrate on the measurement of the first observable wavelength of the bedform. As the telemeter does not allow us to measure continuously the evolution of the bed elevation, we chose to measure the wavelength after given time intervals ($t = 30\,$s, $60\,$s, $\ldots$). Depending on the grain size, it takes more or less time for the ripples to reach a measurable amplitude and wavelength. We were able to extract from the auto-correlation signal of the ripple profile a measurable wavelength at $t = 30\,$s for coarse grains ($d = 500\,\mu$m), and at $t = 1\,$min for fine grains ($d = 250\,\mu$m and $d = 100\,\mu$m), independently of

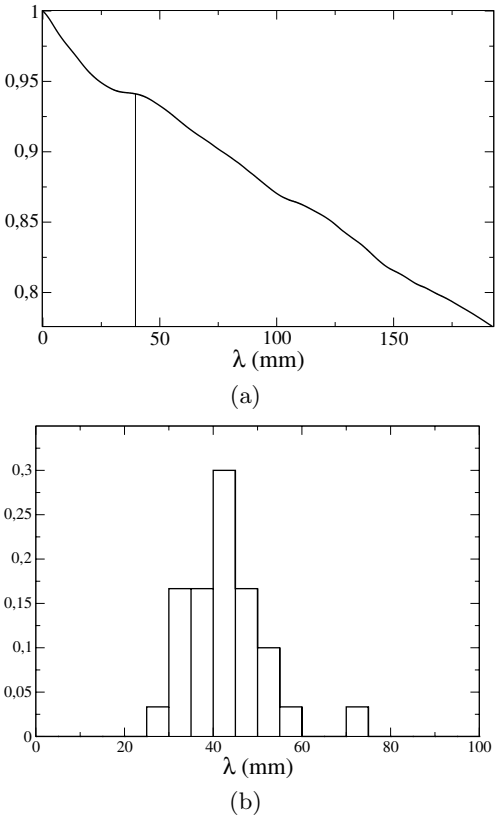

Fig. 7. (a) Auto-correlation of the bed profile measured by telemetry at $t = 1$ min with grains of diameter $d = 250\,\mu$m. A marginal peak appears at $\lambda = 38$ mm. (b) Distribution of wavelengths at the same time.

the flow rate (see Fig. 7). This procedure allows a good reproducibility of the measurement, but presents the inconvenient that, especially for the runs with the fine grains where the wavelength is measured 1 min after the beginning of the erosion process, the ripples might not only grow in height meanwhile but also coarsen. As a consequence, the measured wavelength may be slightly overestimated in comparison with that corresponding to the very first stages of the development of the bedforms.

Figure 8 gathers our results on the first measurement for different values of the flow rate and the grain size. Taking into account the dispersion of measurements, it is impossible, for a given grain size, to conclude on a significative influence of the friction velocity u_τ on the selected wavelength. On the other hand, the mean grain diameter appears to be a more determinant parameter, as can be seen in Figure 9. The initial wavelength increases with increasing grain size. The variation of the dimensionless wavelength λ/d appears to be roughly independent of the particle diameter ($\lambda/d \simeq 100$–150). This finding would require however further confirmation using additional grain sizes. Our observations are relatively consistent with previous experimental results reviewed by Coleman and Melville [15]. They concluded that for a given sediment size, the initial wavelength is relatively insensitive to flow conditions and that the ratio λ/d slightly

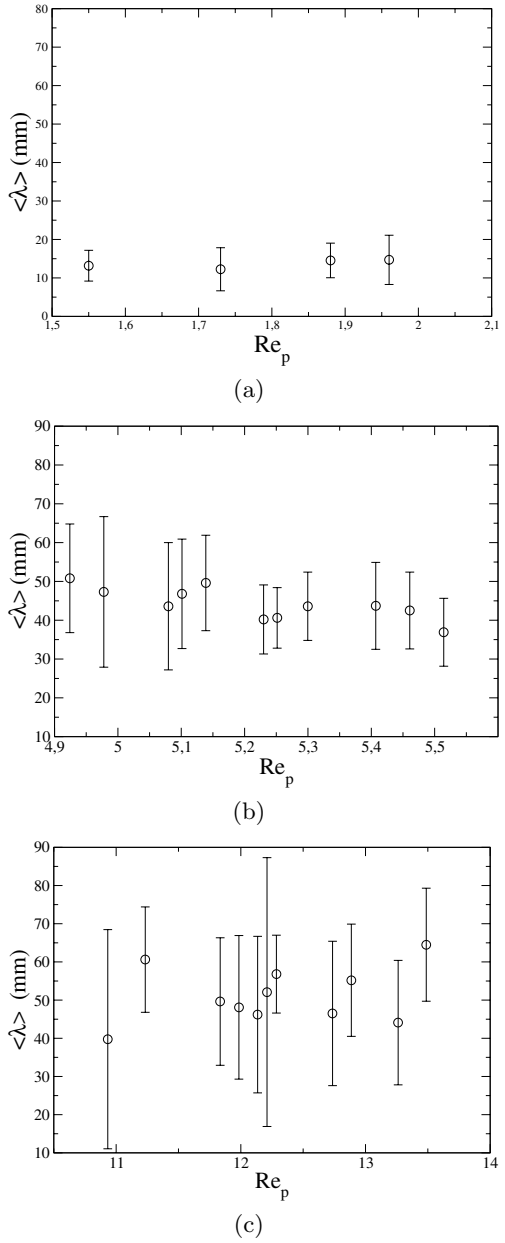

Fig. 8. Average initial wavelength versus the particle Reynolds number, from top to bottom: (a) $d = 100\,\mu$m, (b) $d = 250\,\mu$m and (c) $d = 500\,\mu$m.

decreases with increasing grain diameter (as $d^{-0.2}$). The last finding of Coleman and Melville should be taken with caution, since the dispersion of the collected data is rather large (λ/d varies between 100 and 300 for sediment sizes ranging from 200 to 800 μm).

4 Comparison to theoretical predictions

4.1 Initiation

Our experimental results concerning the initial wavelength of the ripple pattern can be compared to recent theoretical

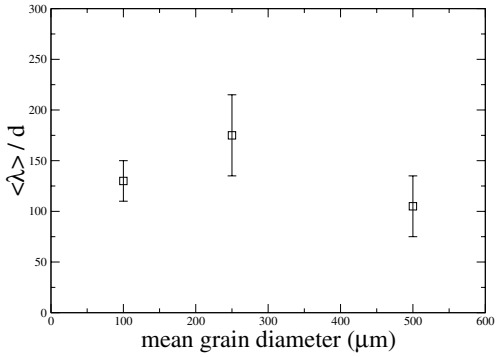

Fig. 9. Variation of the average initial wavelength for different grain sizes.

predictions made by one of the authors [12]. A linear stability analysis was performed to predict the most unstable wavelength of a flat sand bed under a turbulent flow. The mean velocity field above a deformed surface was calculated using an asymptotic matching method [26] and the sand transport dynamics was described in terms of a simple relaxation law which accounts for the fact that the transport rate does not adapt instantaneously to its equilibrium value. The equilibrium sand flux is evaluated using a standard power-law of the Shields number. Within this model, the most unstable wavelength (that is, the mode which is predicted to develop the fastest and then to be observable in the first instants of the instability) scales as the equilibrium length l_{eq}. This length corresponds to the distance needed for an immobile grain to reach equilibrium with the moving fluid. It is the equivalent of the flux saturation length introduced in the description of aeolian sand transport [13,14]. As a first approach, this length has been estimated from the formula giving the drag force on a single sphere. For moderate particle Reynolds numbers (i.e., $1 < Re_p < 10^3$), the predicted wavelength reads then [12]

$$\lambda_{\rm th} \approx 8\, l_{\rm eq} = \frac{\rho_g}{\rho_f} \times \frac{\xi Re_p}{1 + 0.087(\xi Re_p)^{0.75}} \times d \qquad (4)$$

where ξ is a numerical constant relating the equilibrium velocity of the grains to u_τ, ρ_g is the density of the grains and ρ_f that of the fluid. If one takes $\xi = 5$, $Re_p = 15$ and $\rho_f/\rho_s = 2.5$, one finds a wavelength of order of $60\,d$. Furthermore, this formula predicts that λ/d depends on the particle Reynolds number and increases with increasing Re_p. In particular, it means that λ/d should increase with increasing grain diameter. This theory, although it predicts the correct order of magnitude for the ripple wavelength, fails in reproducing the correct dependence on the grain diameter and shear velocity. An effort is therefore required to obtain a better theoretical estimation of the equilibrium length.

In the former theoretical studies, it was generally assumed that the sediment transport rate was, at any time, equal to its equilibrium value. Within this framework, one can cite the predictions of Richards model applicable to turbulent flows [4]. He found that the initial ripple wavelength depends both on the internal friction angle ϕ of the granular material and the hydraulical roughness length z_0 of the bed. In particular, he predicts that the wavelength should scale linearly with z_0. If he adopts the value of $z_0 = d/30$ which is appropriate to surface made rough with fixed grains, his model underpredicts the wavelength by two orders of magnitude. He therefore argued that in the case of erodible bed, the hydraulical roughness is increased due to the bed load layer. Based on the work of Smith et al. [27], he adopted a constant value $z_0 \simeq 4d$, which leads to an estimation of the ratio λ/d of order of 250 for a granular material with an internal friction angle $\phi = 30°$. As a conclusion, this theory, although it apparently predicts the correct scalings, suffers from its extreme sensitivity of the value adopted for the hydraulical roughness z_0, which is not easily accessible to experiments. Further experimental measurements would be therefore required to measure with accuracy the hydraulical roughness of erodible beds and test the validity of Richards hypothesis.

Another important issue should be addressed here. It must be kept in mind that the theoretical predictions are only valid in the linear regime, that is when the amplitude of the ripples is very small and the nonlinear effects are negligible. The experimental estimation of the initial wavelength is subject to caution since it is very difficult, depending on the precision of the apparatus used to measure the bedform topography, to access the wavelength at the very first stages of the development of the ripples. The linear regime is characterized by an exponential growth of the ripple height. Due to the limitations of our set-up, we were unable to exhibit such a regime in our experiments. It is then arguable that the linear regime lasts a very short time before our first measurements. Therefore, the behavior of ripples after long times appears to be an easier parameter to access experimentally, which should encourage theoretical works in this direction.

4.2 Long term evolution

Very few theoretical investigations have been undertaken on the coarsening process of subaqueous ripples. It is necessary to go beyond the linear approximations that are usually adopted for the stability analysis. However, the complete calculation of the fluid flow over a finite-size bedform, for each time step, still requires too much computation time. It is then necessary to make some approximations. Recently, Lagrée [19] performed numerical simulations in the case of a laminar shear flow described by a triple deck model. This calculation only takes into account the non-linearities arising from the transport law (that is, the fluid flow is described in the linear approximation). The simulations show that the existence of a threshold in the transport law is enough to trigger the coarsening process. The wavelength is found to evolve linearly with time, which corresponds to the first regime we observed for large grains (though it must be kept in mind that the fluid conditions are not identical). However, no saturation of the growth is observed (i.e., the wavelength

increases until it reaches the size of the computational domain). Hence, an explanation for the eventual saturation of the wavelength and amplitude, if not directly the presence of the upper wall, has to be found by investigating the non-linearity of the fluid flow.

5 Conclusion and prospects

We presented in this paper the results of an experimental study of sand ripple growth under a steady turbulent water flow. We provide a precise measurement of the flow conditions in the channel used for the ripple experiments. We focused on the first instants of the instability. Measurements of the average initial wavelengths were performed for different values of the grain size and the friction velocity. The initial wavelength is found to depend essentially on the grain diameter but only slightly on the shear velocity. In particular, the wavelength seems to scale linearly with the grain diameter. These observations compare successfully to other experimental data. The theoretical predictions based on linear stability analysis are not fully satisfactory. It is important to stress that the linear approximation is only valid in the first stages of the development of the bedform when the nonlinear effects are negligible. In this linear regime, the growth of the ripple amplitude is expected to be exponential. Experimentally, we were not able to observe this regime probably because it lasts only a very short time and that our set-up did not allow us to measure the ripple amplitude in the very first instants of the instability. This means that the determination of the 'true' initial wavelength (i.e., that corresponding to the linear regime) is difficult. Besides, this suggests that the nonlinear effects come into play very rapidly and that the ripple pattern may coarsen before its amplitude and wavelength become measurable. This poses clearly the problem of the pertinence of the measurement of the initial wavelength which may depend on the vertical resolution of the device used to determine the ripple profile. It is then essential that future theoretical calculations focus not only on the linear regime but also on the coarsening regime.

We also provided results concerning the long-time behavior of the ripples. The evolution of the average amplitude and wavelength were measured during the dynamics of the ripples. We identified the existence of two different coarsening regimes: for the small grains (less than $200\,\mu$m), the amplitude and wavelengths grow logarithmically and no saturation is observed. On the contrary, the ripples made of larger grains ($500\,\mu$m) grow linearly with time, rapidly reaching a saturated state. The small-grain regime (unlimited logarithmic growth) can be compared with the results obtained by Loiseleux et al. [7] whereas the large-grain regime (linear growth with saturation) reminds the observations of Betat et al. [17].

Lastly, we should stress that, as noticed by Kuru et al. [9], the ripples present the same characteristic features in the laminar and turbulent flow regimes. As soon as the nature of transport (i.e., bedload and/or suspension) is the same, the mechanisms seem to be identical. However, even in the simple case of laminar flow, the coarsening process still remains to be correctly modeled and understood. Neither the logarithmic growth nor the saturation observed in our experiments (depending on the grain size) can yet be predicted theoretically or numerically. In particular, the influence of the finite size of the experimental set-up and a better description of the grain transport should be incorporated into future theoretical and numerical studies.

References

1. R.A. Bagnold, *The physics of blown sand and desert dunes* (Chapman and Hall, Londres, 1941)
2. G.M. Kondolf, H. Pieay, *Tools in fluvial geomorphology* (Wiley, Chichester, 2003)
3. B.M. Sumer, M. Bakioglu. Phys. Rev. E **144**, 117 1984
4. K.J. Richards. J. Fluid Mech **99**, 597 1980
5. A.J. Raudkivi. Journ. Hyd. Eng. **123**, 58 1997
6. F. Charru, H. Mouilleron-Arnould. Fluid Mech. **452**, 303 2002
7. T. Loiseleux, D. Doppler, P. Gondret, M. Rabaud. in *Proceedings of the second international workshop on marine sandwaves and river dune dynamics*, p. 200, Enschede, Netherlands, 2004
8. A. Betat, V. Frette, I. Rehberg. Phys. Rev. Lett. **83**, 88 1999
9. W.C. Kuru, D.T. Leighton, M.J. McReady. Int. J. Multiphase Flow **21**, 1123 1995
10. D. Leighton, A. Acrivos. Chem. Engng. Sci. **41**, 1377 1986
11. A. Valance, V. Langlois. Eur. Phys. J. B **43**, 283 2005
12. A. Valance. Eur. Phys. J. B **45**, 433 2005
13. G. Sauermann, K. Kroy, H.J. Hermann. Phys. Rev. E **64**, 031305 2001
14. B. Andreotti, P. Claudin, S. Douady. Eur. Phys. J. B **28**, 341 2002
15. S.E. Coleman, B.W. Melville. J. Hydr. Engng. ASCE **122**, 301 1996
16. M.S. Yalin. J. Hydr. Engng. ASCE **111**, 1148 1985
17. A. Betat, C.A. Kruelle, V. Frette, I. Rehberg. Eur. Phys. J. E **8**, 465 2002
18. J.H. Baas. Sedimentology **46**, 123 1999
19. P.-Y. Lagrée. Physics of Fluids **15**, 2355 2003
20. H. Schlichting, K. Gersten. (Springer, 2000)
21. S.R. McLean. Earth Sci. Rev. **29**, 31 1990
22. V. Langlois, A. Valance. Phys. Rev. Lett. **94**, 248001 2005
23. V. Langlois, A. Valance. Unpublished results
24. J.M. Nelson. Earth Sci. Rev. **29**, 97 1990
25. G. Rousseaux, A. Stegner, J.E. Wesfreid. Phys. Rev. E **69**, 031307 2004
26. P.S. Jackson, J.C.R. Hunt. Quart. J. R. Met. Soc. **101**, 929 1975
27. J.D. Smith, S.R. McLean. J. Geophys. Res. **82**, 1735 1977